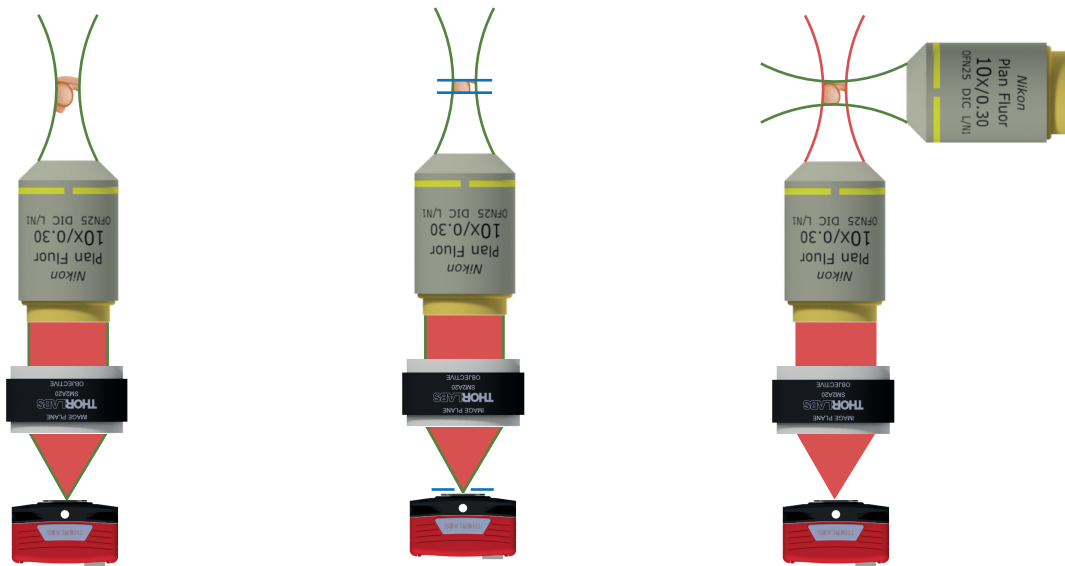


Chapter 2

Contemporary light-sheet technology

Light-sheet Fluorescence Microscopy (LSFM) is revolutionising the way in which complex, living biological samples can be imaged at high spatial and temporal resolution. The technique deviates from conventional epi-fluorescence microscopy in that the sample is illuminated orthogonally to the detection axis. The decoupling of illumination and excitation allows for the construction of light sheets whereby a single plane of interest is excited. As such, the technique offers optical sectioning capability comparable to a confocal microscope whilst still using a wide-field detection system [1–3].

This garners two key advantages: firstly, as the plane of interest being detected is irradiated, the incident photon dosage is drastically reduced and so photo-toxicity to the sample is minimised. This is in stark contrast to confocal imaging where signal is collected from a small voxel along the illumination axis whilst the entire sample is illuminated when recording a single image plane. Secondly, wide-field detection enables a significant temporal resolution increase in LSFM versus confocal. For rapid volumetric imaging of complex organisms LSFM is becoming the technique of choice in developmental biology [4–9], plant science [10] and cell biology [11, 12].



(a) Widefield imaging, epi-fluorescence; without optical sectioning

(b) Confocal imaging using a pin-hole at the imaging plane; epi-fluorescence, optical sectioning

(c) Widefield imaging with orthogonal illumination using a light-sheet; optical sectioning

Fig. 2.1 Light-sheet microscopy (c) combines the fast wide-field imaging capabilities of epi-fluorescence microscopy (a) with the optical sectioning capabilities of confocal microscopy (b).

The concept of orthogonal detection and illuminations dates back to 1903 when Zsigmondy and Siedentopf studied colloids in their *ultra-microscope* [1]. Technological advances in fluorescent dyes, labelling and digital image detection permitted Voie *et al.* [2] to present the first light sheet fluorescence microscope in 1993. By 2004 Huisken *et al.* [3] demonstrated the potential of LSFM for *in-vivo* imaging with cellular resolution.¹

2.0.1 Light-sheet generation

2.0.2 Optical light-sheet generation

Huisken *et al.* were seminal in their usage of Gaussian laser emissions for the generation of their light sheets despite Gaussian beams have a distinct trade-off when used in LSFM applications, in that the thinner the light sheet the narrower the usable field of view. Equation (2.1) models the Gaussian beam approximation where

¹Design choices made here have heavily influenced the openSPIM project, an information toolkit found on the internet for constructing a LSFM

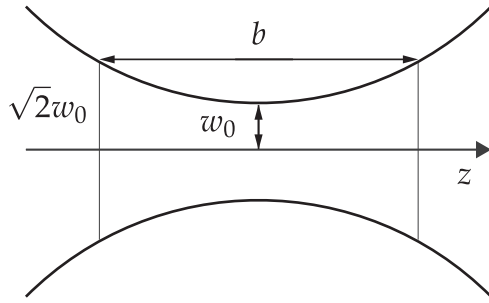


Fig. 2.2 Schematic of the propagation of a Gaussian beam. The beam is assumed to be collimated (par-axial) within the length b (the confocal parameter) for a given spot size w_0 . The spreading of the beam obeys a Lorentzian hyperbole as in Equation (2.2)

the Full-Width at Half-Maximum (FWHM) ($\sqrt{\ln(2)}w(z)$) increases as a Lorentzian (Equation (2.2)) when a distance z away from the focal plane depicted in Fig. 2.2. The rate at which this occurs is dependent on the Rayleigh length in Equation (2.3) which quantifies the trade-off. The confocal parameter ($b = 2z_R$) is a metric for the distance over which a Gaussian beam propagates as if it were parallel (neither converging nor diverging). For LSFM this is the distance over which the light-sheet can be assumed to be of homogeneous thickness.

Huisken *et al.* also pioneered the use of a cylindrical lens to focus the Gaussian beam along one dimensional into a Gaussian light-sheet. For LSFM, the Gaussian intensity profile of a Gaussian beam requires that the excitation beam is over expanded and later cropped by an aperture to create a homogeneous illumination profile. The procedure is optically lossy, but, laser intensity is typically in surplus for fluorescence microscopy techniques; a good fluorescent sample needs 2 ± 1 mW in comparison to a low end diode laser emitting 100 mW+.

$$I(r, z) = I_0 \left(\frac{w_0}{w(z)} \right)^2 e^{\frac{-2r^2}{w(z)^2}} \quad (2.1)$$

$$w(z) = w_0 \sqrt{1 + \frac{z}{z_R}} \quad (2.2)$$

$$z_R = \frac{\pi w_0^2}{\lambda} \quad (2.3)$$

Where z_R is the Rayleigh length; w_0 is the spot of size of the beam and λ is the wavelength of light.

2.0.3 Digital light-sheet generation

Keller *et al.* [13] proposed sweeping a narrow laser beam through the sample to create a virtual light-sheet. This was achieved by oscillating galvanic mirrors at kHz frequencies, well over the Nyquist limit in comparison to the imaging acquisition rate [13]. To ensure a homogeneous illumination and distributed photon dosage a tele-centric $f\theta$ lens was used to convert beam angle optically from the scanning mirrors in to a linear position ².

Using Digitally scanned Light-sheet Microscopy (DSLM) instead of a cylindrical lens based system offers some key advantages. Firstly, as the beam is scanned rather than optically stretched there can be no optical interference of coherent photons between neighbouring regions in the sample, this reduces speckles and shadows. Secondly, illumination intensity can be modulated such that structure can be superimposed on the sample giving the potential for super-resolution image improvement. This resolution improvement has so far solely been experimentally demonstrated in the direction of the the scanning due to geometrical constraints [14].

2.0.4 Volumetric imaging

The true value of LSFM is in its capability to perform fast volumetric imaging. Huisken's original Selective Plane Imaging Microscope (SPIM) required the samples to be scanned mechanically through the static light sheet, potentially perturbing the sample, depending on the speed of the scanning. DSLM improves upon the static light-sheet by using a second galvanometric mirror to move the light-sheet relative to the static sample, the detection objective is then mounted on a high speed and precision axial translator and tuned to follow the light-sheet. Ideally, piezoelectric actuators are used as their settling times are on the order of milliseconds providing speed and accuracy needed to match 100 Hz cameras.

Remote focusing

With DSLM, instead of the sample motion causing a disturbance a large objective local to the specimen is causing turbulence. This mechanical motion was replaced by placing an Electronically Tuneable Lens (ETL) [15] in the detection path. The ETL was used to shift the working distance of the detection objective to match the

²A practice borrowed from laser scanning microscopy.

scanning light-sheet. The technique suffers from fluorescent signal losses in the further four lenses and two mirror surfaces required ($\sim 80\%$ signal retrieved). ³ The technique is also prone to spherical aberration, and is a more involved method as the system requires a non-linear calibration. Huisken *et al.* showed, using a contrast grid, that image quality and aberrations are negligibly affected; then proceeded to produced 100 Hz volumetric imaging, though on small volumes [16]. Disaspro *et al.* improved upon using ETLs by optically relaying a virtual image of the sample and using a secondary microscope, with an actuated objective; the result was interia-free imaging and fewer optics and ETL-induced aberrations [17].

2.1 Objective arrangements

2.1.1 Single view imaging

Light-sheet microscopes are distinct in that two objectives are used orthogonally causing the technique to incompatible with most standard epi-fluorescence biological mounting practices. Efforts have been made to make light-sheet imaging more compatible through novel objective arrangements as well as intuitive mounting approaches.

Horizontal orientation

Huisken *et al.*, for instance, mounted two objectives in a horizontal configuration; a detection objective built into a sample chamber and illuminated using a light-sheet through a clear window [18]. This configuration was chosen so that a sample could be lowered into the system and, crucially, rotated without gravity causing registration errors when reconstructing the volume tomographically, see Fig. 2.3a. Rotational volumetric imaging also minimises shadows and improves image quality lost to scattering especially in thick $>500\text{ }\mu\text{m}$ samples as in Fig. 2.3b. Mounting a sample from below and rotating produces the same result but requires a more sophisticated chamber design to contain the sample medium. A horizontal geometry is important for imaging plant biology, as the objectives do not inhibit the plant's natural tendency to grow upright [19].

³The mirrors are used to ensure the ETL is horizontal to gravity as further aberrations occur if the tunable surface is not entirely flat. Two mirrors from the tunable light sheet could be removed by using mechanically deforming tunable lenses instead of electro wetting tunable lenses.

Vertical orientation

An alternative to the horizontal configuration is mounting the detection objective above the sample, and then illuminating the sample from the side. A vertical orientation is attractive as it can be compatible with commercial optical microscopes as well the chamber not requiring an inbuilt detection objective [ALEKS 29 30]. Both of these techniques can allow for an additional illumination objective with counter-propagating illumination. By offsetting the foci of the illumination objectives along the axis of propagation an overall more homogenous illumination profile can be created, with reduced shadows.

45° orientation

Shroff *et al.* then pioneered use of two objectives in a V configuration above the sample through inverted Selective-Plane Imaging Microscope (iSPIM). With choice objectives, whereby the sum of the opening angles of both objectives does not exceed 180°, samples prepared with standard mounting procedures may be imaged in a petri-dish or glass slides [20].

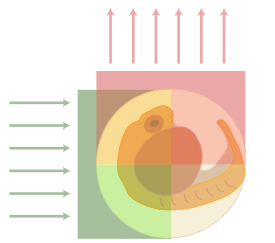
Optimal orientation

In a bid to maximise sample accessibility and numerical aperture, Betzig *et al.* [14] commissioned a high NA (0.6) custom excitation objective to fit with the high NA (1.1) Long Working Distance (LWD) detection objective (Nikon CFI75). A custom excitation objective was needed as high NA objectives are physically large with short working distances. In mounting the orthogonal pair at an angle such that they were planar so a flat surface, Betzig *et al.* maximised detection and excitation NA whilst minimising sample mounting impedance.

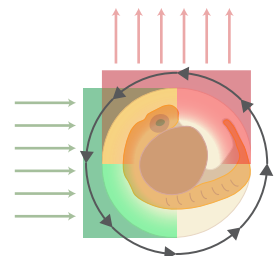
2.1.2 Multi-view

Shroff *et al.* introduced alternate imaging between each objective of the iSPIM in the form of the dual inverted Selective-Plane Imaging Microscope (diSPIM) [24], depicted in Fig. 2.3e. ⁴ Axial resolution that would otherwise be lost to thick light-sheets is recovered by switching the imaging and detection arms. The two data sets captured by each camera are fused in post processing to provide near isotropic

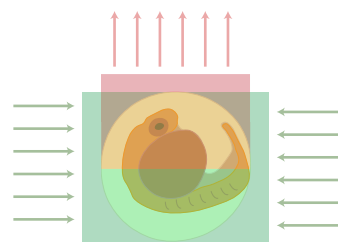
⁴This system is now a commercial light-sheet solution provided by ASI.



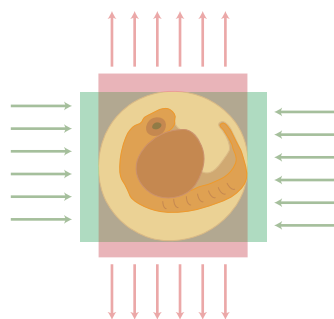
(a) Single detection, single illumination [21]



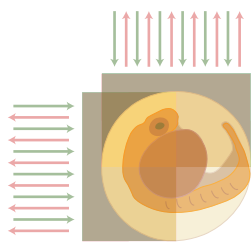
(b) Single detection, single illumination, with sample rotation [22]



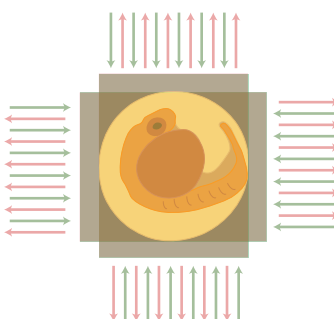
(c) Single detection, dual illumination



(d) Dual detection, dual illumination [23]



(e) Single detection, single illumination, with alternate illumination and detection [24]



(f) Dual detection, dual illumination, with alternate illumination and detection

Fig. 2.3 Schematic of objective lens arrangements for optical light-sheet imaging. (a) and (b) both use a single objective lens for imaging and illumination, with (b) rotating the sample so that optimal imaging is not limited to the *optimal quarter* (yellow). (c) adds an additional illumination objective to mitigate illumination light lost through sample penetration. (d) adds a further imaging objective lens to mitigate detected light being lost to sample penetration; the images of each detecting objective are later computationally fused. (e) uses a pair of illumination and detection lenses to enhance the resolution (deeper yellow) in the *optimal quarter*, by fusing the data from each objective alternately. (f) repeats the imaging and illumination alternation approach from (e) but does so in four objectives instead of two. **Image acquisition speeds** (b), (c) and (d) are the same speed as (a) but (d) requires a computational reconstruction in post-processing. (e) is half the speed of (a) and (f) is a quarter the speed of (a), both requiring extensive post-processing computation.

three dimensional resolution. Where LSFM provides the most improvement over other techniques, such as in large, thick biological samples; scattering induced image degradation then becomes significant, both for excitation and emission light. For imaging in thick samples using orthogonal detection and excitation there does exist an *optimal quarter* (see Fig. 2.3) wherein excitation and emission photons are the least scattered.

Krzic *et al.* used the horizontal orientation of Huisken's SPIM, in Multiview Selective-Plane Illumination Microscope (MuVi-SPIM) (Fig. 2.3d) where two excitation and two detection objectives were packed around a hanging sample [23]. MuVi-SPIM is able to image all regions of the sample. To minimise gross sample scattering, sample rotation is necessary. Acquiring volumes via rotational tomographically raises further unique issues such as volume registration, rotational synchronisation and longer acquisition times.

2.2 Single objective light-sheet microscopy

Prior to refinements in objective positioning from the last section, Dunsby *et al.* conceptualised a system for single objective light-sheet microscopy.⁵ Dunsby *et al.* proposed illuminating the sample using a high NA objective whereby the light-sheet would illuminate at an oblique angle to the optical axis, the detected signal is then retrieved using the same objective [25]. Optically, the sample is conjugated to a virtual position where a pair of objectives (excitation and detection) analyse the

⁵The advent of such systems could provide a plug-and-play light-sheet experience on commercial microscope frames.

virtual sample in a conventional light-sheet manner. The technique suffers in that only half the imaging NA may be collected. Oblique Plane Microscopy (OPM) is an involved technique as it requires that a light-sheet microscope is constructed, behind an optical relay system, relaying the virtual image from a standard microscope body.

Swept Confocally-Aligned Planar Excitation (SCAPE) uses the same principle as OPM but attempts to greatly reduce the optics and labour required. Hillman *et al.* do so by using a single polygonal mirror in the infinity space of the detection objective to redirect excitation and emission light [26]. The polygonal mirror then rotates to sweep the light-sheet and detecting focal plane through the sample.

Virtual sample manipulation is alluring as virtual manipulations can be performed that are impossible physically. Zhang *et al.* [27] created a virtual sample using a similar relay system to Dunsby *et al.*, but crucially they positioned an atomically flat mirror which rotated their virtual sample by 90°. In doing so, the real sample could be illuminated along the optical axis and the mirrored virtual projection was imaged directly onto a camera.

Using small mirrors near the sample is another viable, though more restrictive, approach to single objective LSF. Galland *et al.* fabricated micro-wells with 45° micro-mirrors [28], converting any commercial scanning microscope into a light-sheet microscope.⁶ Both techniques limit the size of the sample and their sectioning capability heavily depends on the quality of the mirrors used.

Ploschneret *et al.* minimised the size of the second excitation objective rather than remove it by substituting it for a multimode fibre [29]. By assuming that a multi-mode fibre operates deterministically on an input light source, Ploschneret *et al.* were able to homogenise the illumination output of the fibre using an Spatial Light Modulator (SLM). They then demonstrated the exotic beam profiles using the same SLM.

2.3 Illumination

Novel illumination techniques have been proposed in a bid to circumvent the ubiquitous Gaussian beam extension to sheet thickness trade-off and minimising shadowing artefacts.

⁶Leica produce a similar solution in the form of an objective adapter which holds two mirrored surfaces near the sample creating a similar effect.

2.3.1 Gaussian techniques

Santi *et al.* proposed using a Gaussian sheet with a narrow FOV, scanning the sample and stitching the result [30]. A final image can then be fused to achieve maximum axial resolution though with a direct cost for time of acquisition and photobleaching versus axial resolution, with an exceptionally high NA light sheet tending to becoming as slow and damaging as a confocal system.

Fu *et al.* proposed the superposition of multiple thin and focally-offset Gaussian light-sheets to create a tiling effect without the loss of temporal resolution [31]. The tiling effect was produced by using an SLM whose hologram had multiple lens-like (quadratic) phase patterns superimposed. The technique suffers from the additional photo-dosage imparted from the undesirable lobes of the Gaussian beam, moreover these low axial-resolution sections also contribute fluorescent background reducing the net Signal to Noise ratio (SNR) of the system.

In multidirectional Selective Plane Illumination Microscopy (mSPIM) Huisken *et al.* added an additional scanning mirror to control the emission angle of the light-sheet. By dithering this mirror slightly during an acquisition shadowing artefacts were markedly reduced [32], see Fig. 2.4.

2.3.2 Exotic beams

Species of exotic beam do exist and whose properties do not subscribe to classical Gaussian beam limitations.

2.3.3 Bessel beams

Bessel beams are non-diffracting and self-healing; meaning they produce thin long beams as well reconstruct behind occlusions, making them very desirable for light-sheet applications. They can be optically constructed from either an axicon lens or a amplitude mask with a annular ring opening, the latter being inexpensive but the most optically lossy. Unlike Gaussian beams the extension and thickness of a theoretical Bessel beam can be entirely decoupled, in practice a Bessel beams only behave as such over short distances [33] of up to $\sim 30 \mu\text{m}$. Bessel beams, however, suffer from having multiple undesirable outer orders; the more ideal a Bessel beam is, the closer the ratio of the energy of the central beam versus outer lobes is to 1. As such, a singular scanned Bessel beam causes a significant background

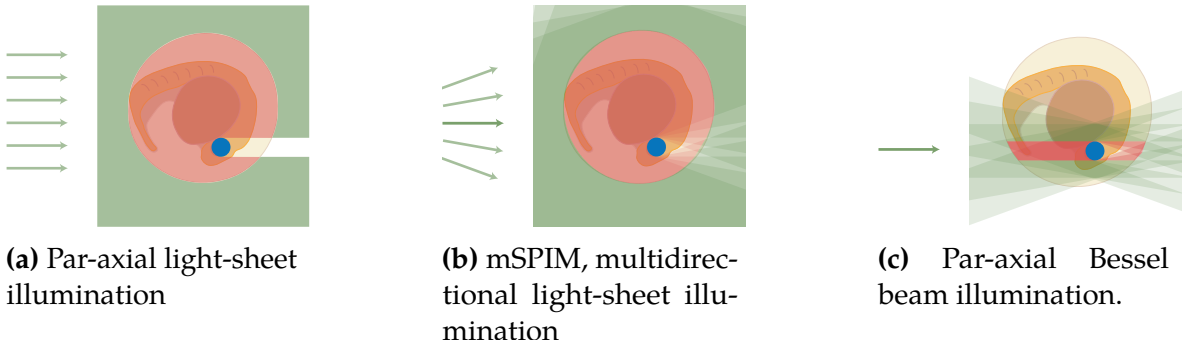


Fig. 2.4 Shadowing artefacts in light-sheet(a) can be mitigated through different types of illumination. (b) uses light-sheets from multiple directions to illuminate behind an occlusion. (c) uses Bessel sheets which have the property of self-healing behind occlusions; this happens as Bessel beams arise from constructive interference from angled plane waves

signal. Betzig *et al.* exploited these additional orders by constructing multiple Bessel beams in the scanning plane [14]. The spacing of which was controlled by varying the periodicity of the sinusoidal amplitude pattern (diffraction grating) on an annular amplitude mask (Bessel beam mask). In doing so the, undesirable orders constructively interfered to reinforce the zeroth orders of the parallel beams. Finally, they tuned the periodicity lattice light-sheet such that the outer orders above and below the scanning plane lay at the first minima in the detection Point Spread Function (PSF) reducing the net fluorescent axial background.

Airy Beams

Airy beams also self-heal similarly to Bessel beams but are more extended comparatively. Airy beams are constructed using a coma-like (cubic) phase pattern and exhibit a characteristic beam curvature. The curvature produces an asymmetric profile along the detection axis, which then needs to be deconvolved in post-processing. Vettenburg *et al.* demonstrated a similar axial resolution improvement as with Bessel beams, whilst achieving a ~ 3 increase in FOV [34].

2.3.4 Thinner sheets

By exploiting the quantum mechanical nature of fluorophores, methods for further improving sheet thickness have included using Simulated Emission Depletion (STED) and 2-Photon (2P) excitation. Using an addition laser to deplete the excitation sheet (using STED) out of plane fluorescence can narrow a Gaussian light sheet

to $<1\text{ }\mu\text{m}$ [35]. 2P light-sheet microscopy uses the the narrowing effect of 2P (Section 1.3.2) excitation to create a narrow excitation sheet.

2.4 Summary

Light-sheet microscopy can be used to produce fast volumetric data. Typically this achieved with two orthogonal objectives, each for excitation and detection. Having multiple objectives near a biological sample does however impede traditional mounting strategies. Classical light-sheets have a dependancy between their FOV and axial thickness, these constraints can be overcome with exotic illumination modalities.

The techniques and methods presented here for generating light-sheets and detecting the resultant fluorescence, in thick biological samples, will be used in the following chapter to inform the design of a 3D-particle tracking light-sheet microscope.

References

1. Siedentpf, H & Zsigmondy, R. Über Sichtbarmachung und Groessenbestimmung ultramikroskopischer Teilchen, mit besonderer Anwendung auf Goldrubbingsern. *Annalen der Physik* **10**, 1–39 (1903).
2. Voie, A. H., Burns, D. H. & Spelman, F. A. Orthogonal-Plane Fluorescence Optical Sectioning: Three-Dimensional Imaging of Macroscopic Biological Specimens. *Journal of Microscopy* **170**, 229–236 (1993).
3. Huisken, J., Swoger, J., Bene, F. D., Wittbrodt, J. & Stelzer, E. H. K. Optical Sectioning Deep Inside Live Embryos by Selective Plane Illumination Microscopy. *Science* **305**, 1007–1009 (2004).
4. Keller, P. J. *et al.* Fast, high-contrast imaging of animal development with scanned light sheet-based structured-illumination microscopy. *Nature methods* **7**, 637–42 (2010).
5. Verveer, P. J. *et al.* High-resolution three-dimensional imaging of large specimens with light sheet-based microscopy. *Nat Meth* **4**, 311–313 (2007).
6. Mickoleit, M. *et al.* High-resolution reconstruction of the beating zebrafish heart. *Nature methods* **11**, 1–6 (2014).
7. Ichá, J. *et al.* Using Light Sheet Fluorescence Microscopy to Image Zebrafish Eye Development. *Journal of Visualized Experiments* (2016).
8. Keller, P. J. & Ahrens, M. B. Visualizing Whole-Brain Activity and Development at the Single-Cell Level Using Light-Sheet Microscopy. *Neuron* **85**, 462–483 (2015).

9. Ichikawa, T. *et al.* Live imaging and quantitative analysis of gastrulation in mouse embryos using light-sheet microscopy and 3D tracking tools. *Nature protocols* **9**, 575–85 (2014).
10. Wangenheim, D. V. *et al.* Rules and Self-Organizing Properties of Post-embryonic Plant Organ Cell Division Patterns. *Current Biology*, 1–11 (2016).
11. Capoulade, J., Wachsmuth, M., Hufnagel, L. & Knop, M. Quantitative fluorescence imaging of protein diffusion and interaction in living cells. *Nature Biotechnology* **29**, 835–839 (2011).
12. Cella Zanacchi, F. *et al.* Live-cell 3D super-resolution imaging in thick biological samples. *Nature Methods* **8**, 1047–1049 (2011).
13. Keller, P. J. & Stelzer, E. H. Quantitative in vivo imaging of entire embryos with Digital Scanned Laser Light Sheet Fluorescence Microscopy. *Current Opinion in Neurobiology* **18**, 624–632 (2008).
14. Chen, B.-C. *et al.* Lattice light-sheet microscopy: Imaging molecules to embryos at high spatiotemporal resolution. *Science* **346**, 1257998–1257998 (2014).
15. Fahrbach, F. O., Voigt, F. F., Schmid, B., Helmchen, F. & Huisken, J. Rapid 3D Light-Sheet Microscopy with a Tunable Lens. *Optics Express* **21**, 21010–21026 (2013).
16. Fahrbach, F. O., Voigt, F. F., Schmid, B., Helmchen, F. & Huisken, J. Rapid 3D Light-Sheet Microscopy with a Tunable Lens. *Optics Express* **21**, 21010–21026 (2013).
17. Duocastella, M. *et al.* Fast Inertia-Free Volumetric Light-Sheet Microscope. *ACS Photonics* **4**, 1797–1804 (2017).
18. Huisken, J., Swoger, J., Bene, F. D., Wittbrodt, J. & Stelzer, E. H. K. Optical Sectioning Deep Inside Live Embryos by Selective Plane Illumination Microscopy. *Science* **305**, 1007–1009 (2004).

19. Wangenheim, D. V. *et al.* Rules and Self-Organizing Properties of Post-Embryonic Plant Organ Cell Division Patterns. *Current Biology*, 1–11 (2016).
20. Kumar, A. *et al.* Dual-View Plane Illumination Microscopy for Rapid and Spatially Isotropic Imaging. *Nature protocols* **9**, 2555–73 (2014).
21. Wu, Y. *et al.* Inverted Selective Plane Illumination Microscopy (iSPIM) Enables Coupled Cell Identity Lineaging and Neurodevelopmental Imaging in *Caenorhabditis Elegans*. *Proceedings of the National Academy of Sciences* **108**, 17708–17713 (2011).
22. Huisken, J., Swoger, J., Bene, F. D., Wittbrodt, J. & Stelzer, E. H. K. Optical Sectioning Deep Inside Live Embryos by Selective Plane Illumination Microscopy. *Science* **305**. bibtex: huisken_optical_2004-1, 1007–1009 (2004).
23. Krzic, U., Gunther, S., Saunders, T. E., Streichan, S. J. & Hufnagel, L. Multiview Light-Sheet Microscope for Rapid *in Toto* Imaging. *Nature Methods* **9**, 730–733 (2012).
24. Kumar, A. *et al.* Dual-View Plane Illumination Microscopy for Rapid and Spatially Isotropic Imaging. *Nature protocols* **9**, 2555–73 (2014).
25. Dunsby, C. Optically Sectioned Imaging by Oblique Plane Microscopy. *Optics Express* **16**, 20306 (2008).
26. Bouchard, M. B. *et al.* Swept Confocally-Aligned Planar Excitation (SCAPE) Microscopy for High-Speed Volumetric Imaging of Behaving Organisms. *Nature Photonics* **9**, 113–119 (2015).
27. Li, T. *et al.* Axial Plane Optical Microscopy. *Scientific Reports* **4**, 7253–7253 (2014).
28. Galland, R. *et al.* 3D High- and Super-Resolution Imaging Using Single-Objective SPIM. *Nature Methods* **12**, 1–13 (August 2014 2015).
29. Plöschner, M. *et al.* Multimode fibre: Light-sheet microscopy at the tip of a needle. *Scientific Reports* **5**, 18050–18050 (2015).

30. Santi, P. A. *et al.* Thin-Sheet Laser Imaging Microscopy for Optical Sectioning of Thick Tissues. *BioTechniques* **46**, 287–294 (2009).
31. Fu, Q., Martin, B. L., Matus, D. Q. & Gao, L. Imaging Multicellular Specimens with Real-Time Optimized Tiling Light-Sheet Selective Plane Illumination Microscopy. *Nature Communications* **7**, 11088–11088 (2016).
32. Huisken, J. & Stainier, D. Y. R. Even Fluorescence Excitation by Multidirectional Selective Plane Illumination Microscopy (mSPIM). *Optics Letters* **32**, 2608–2610 (2007).
33. Gao, L., Shao, L., Chen, B.-C. & Betzig, E. 3D live fluorescence imaging of cellular dynamics using Bessel beam plane illumination microscopy. *Nature protocols* **9**, 1083–101 (2014).
34. Vettenburg, T. *et al.* Light-sheet microscopy using an Airy beam. *Nature methods* **11**, 541–4 (2014).
35. Friedrich, M., Gan, Q., Ermolayev, V. & Harms, G. S. STED-SPIM: Stimulated Emission Depletion Improves Sheet Illumination Microscopy Resolution. *Bioophysical Journal* **100**, L43–L45 (2011).